THE PRODUCTION OF NEUTRONS BY SECONDARY PROCESSES IN THE PROTON BOMBARDMENT OF DEUTERIUM

by

Yun I. Ssu

---oOo---

A THESIS SUBMITTED IN PARTIAL FULFILMENT OF

THE REQUIREMENTS FOR THE DEGREE OF

MASTER OF SCIENCE

in the Department

of

PHYSICS

We accept this thesis as conforming to the standard
required from candidates for the degree of
MASTER OF SCIENCE

Member of the Department of Physics

THE UNIVERSITY OF BRITISH COLUMBIA

September, 1955

ABSTRACT

Several simple and rugged neutron detecting scintillation counters have been built. The counters consisted of many layered lucite and zinc sulfide powder sandwiches placed on the end of Dumont 6292 photomultipliers.

One of these counters was used to measure the yield and angular distribution of neutrons produced by the bombardment of heavy ice with 1.5 Mev protons (below the D(p,n)2p threshold). The angular distribution of the neutrons was found to be somewhat anisotropic and to depend on target thickness, the anisotropy increasing with target thickness.

It is proposed that the neutron production is due to a double process; deuterons after being struck by incident protons collide with further deuterons in the target producing D(d,n)He^3 neutrons. This proposal has been confirmed by comparison of the experimental results with calculations for thin and thick targets of the yield and angular distribution of neutrons to be expected from the double process. A further confirmation has been obtained experimentally by observing that the yield of neutrons is proportional to the square of the D_2O concentration in mixed D_2O and H_2O targets.

ACKNOWLEDGEMENTS

It is a pleasure to acknowledge the guidance of Dr. J.B. Warren who suggested and kindly supervised the work described herein.

The author is indebted to Dr. D.B. James and Dr. K. Erdman for advice and encouragement and to Mr. G.B. Chadwick and Mr. C. Neilson for their help with the experimental part of the work. Thanks are also due to the members of the Van de Graaff team for assistance during the runs, in particular to Mr. J.B. Elliott, and to Dr. G.M. Griffiths for help in the preparation of this thesis.

TABLE OF CONTENTS

LIST OF ILLUSTRATIONS

Chapter I

INTRODUCTION

While studying the $D(p,\gamma)He^3$ reaction Warren and Griffiths found that the angular distribution of γ-radiation from this reaction has the form $\mathrm{Sin}^2\theta+C$, where C is a small constant equal to 0.046 for 1 Mev protons and 0.025 for 1.75 Mev protons. In 1952 Wilkinson, using the photodisintegration of the deuteron as a polarization analyzer, found that the γ-radiation is predominantly polarized at 90° to the plane containing the direction of the incident protons. The simplest assumption consistent with the angular distribution and the polarization is that the transition is electric dipole in nature. According to direct radiative capture theory, with conservation of the z-component of the angular momentum as a result of no spin-orbit coupling, Blatt and Weisskopf's formula would give an angular distribution of the form $\sin^2\theta$ for capture of a p-wave proton. The small additional isotropic component represented by "C" above can be explained by adding a small spin-orbit coupling interaction.

Preliminary experiments led Warren and Griffiths to suggest that neutrons accompanied the γ-rays from the $D(p,\gamma)He^3$ reaction. However, the simple lucite and zinc sulfide phosphor combination used by them was not sufficiently sensitive and Boron trifluoride counters were too bulky and γ-ray sensitive to study this effect. In order to correctly evaluate C accurately, it was necessary to study the neutrons further.

The objectives of the present research were (1) to build a highly sensitive neutron detector which must be completely insensitive to γ-radiation, (2) to measure the neutron yield accompanying the $D(p,\gamma)He^3$ reaction and (3) to explain their origin if neutrons were actually found. The only previous work on this subject is described by Jennings et al (1950) in an unpublished Westinghouse report. They measured the excitation curve of neutron production from a thick D_2O target, with a Boron trifluoride counter, and suggested that the neutrons were due to deuterons in the target being scattered by incident protons and then colliding with other deuterons producing $D(d,n)He^3$ neutrons. These authors made an approximate calculation by considering the target in 500 kev-thick layers and the result agreed to an order of magnitude with what they found experimentally, assuming the neutrons were emitted isotropically.

The direct process $D(d,n)2P$ is energetically impossible at the energies under consideration and the cross-section of the photodisintegration of the deuteron is too small to account for the observed yield. The double process suggested by Jennings et al is the most promising theory, and as will be seen later it explains most features of the present experiments, including the fact that the angular distribution is rather anisotropic.

The problem of the neutron yield when a heavy ice target is bombarded with protons has been attacked in several ways. First, an excitation function for neutron production was obtained for protons in the energy range 600 Kev to 1.8 Mev. Second, an experimental measurement of the yield and angular distribution of neutrons was made for 1.5 Mev protons and this was compared with the yield and angular distribution results obtained by a calculation based on the double process hypothesis. Finally, a measurement was made of the yield of the neutrons as a function of the concentration of D_2O in a mixed heavy water and light water target. If the neutron production is due to a direct reaction the yield will be directly proportional to the concentration. However, if a double process is involved the yield should be proportional to the square of the concentration. This follows from the fact that the number of recoiling deuterons is proportional to the concentration of deuteron atoms present in the target, and the chance of a collision between a recoiling deuteron and a further deuteron is also proportional to the concentration of deuteron atoms in the target. As suggested by Mr. G. Chadwick, if the double process mentioned above is the correct one there should be no neutron yield when an ordinary water target is bombarded by deuterons. However, this suggestion was not tried out experimentally due to the high neutron background that would result from the deuteron beam in the Van de Graaff generator.

Chapter II

FAST NEUTRON COUNTERS

1. BF_3 Enriched Long Counter

A BF_3 long counter (Hanson and McKibben 1947, Heiberg 1954) has been used in this investigation. However, since the BF_3 filled counter is most efficient for thermal neutrons it is necessary to surround the counter with several inches of paraffin if it is used to count fast neutrons. Also if it is to be relatively insensitive to a slow neutron background it is necessary to cover the paraffin with cadmium and to surround this with a further paraffin shield on all sides except that from which the fast neutrons enter. Consequently the BF_3 long counter is rather bulky and cannot be placed very close to the target. The counter used here was half a meter long and 40 cms. in diameter. Further the long counter is slightly γ-ray and slow neutron sensitive, so that when placed close to the target under the Van de Graaff generator the γ-ray and scattered neutron fluxes produce a rather high background count. Therefore a counter with much lower sensitivity to γ-rays and slow neutrons was essential for these experiments. The BF_3 counter has, however, proved useful as a monitor for d on d angular distribution runs done to check the characteristics of the counter described later. It was also used for the thick target runs for the p on d experiment where the neutron yield was relatively high, to give an independent check on the identity of the emitted neutrons as well as for the angular distribution measurements. For these experiments an Atomic Instrument Company type 205-B low noise linear preamplifier was used with the long counter in order to get the best possible signal to noise ratio. The preamplifier output was connected to an Atomic Instrument Company type 204 B linear amplifier followed by a discriminator and scaler. The BF_3 counter was operated at 1750V from a stabilized H.T. supply.

2. <u>Zn S-Plastic Fast Neutron Counter</u>

Chadwick (1932) first recognized the existence of the neutron as such, as a result of measurements with a thin window ionization chamber which detected protons which were ejected from a paraffin-wax plate by the incident neutrons. Since that time several instruments have been employed for neutron detection, which used the same principle with various refinements. A simple extension of Chadwick's method is that used by Coon and Nobles (1947) who placed a thin hydrogen containing radiator inside a proportional counter. High pressure hydrogen filled ionization chambers in which the recoil protons are ejected from the chamber gas itself have also been used (Stafford, 1948). With the advent of the scintillation counter, it has become possible to use solid hydrogen containing crystals to detect neutrons by means of the knock-on protons producing light in the crystal, (Bell, 1948, Segel et al, 1954). However, such organic phosphors are also γ-ray sensitive, which prohibits neutron measurements in the presence of large γ-ray fluxes. The γ-ray sensitivity can be considerably reduced by using a very thin layer of an organic phosphor such as Anthra~~s~~cene, since the range of an electron is much greater than that of a proton of the same energy. Several tests were made by the author of thin anthra~~s~~cene films, and it was found that they were not satisfactory for the present experiments, since the neutron detection efficiency is too low when the film is thin enough to have low γ-ray sensitivity.

A thin layer of zinc sulphide powder placed on the end of a photomultiplier can also be used to count the recoil protons from a plastic radiator placed in front of the photomultiplier. However, the combination has low efficiency. An improvement in efficiency was obtained by Hornyak (1952) who mixed Zns powder with lucite molding powder and compressed the mixture under heat to form a solid semitransparent button which was used as a neutron detector. With the bias at which the γ-ray sensitivity is quite low, the device has a neutron efficiency of 2.5%. The useful size is limited by the rather poor transparency. The same idea has been applied by Seagondollar et al (1954) who mixed the Zns powder with Bio-plastic. Emmerich (1954) placed 0.125 inch sheets of lucite in a Zns-paraffine mixture block to act as light guides; with this arrangement he achieved an efficiency of 3.8% for 4 Mev neutrons at a bias level where the efficiency for radium γ-rays was of the order of 10^{-4}. The efficiency of these devices can be improved somewhat by the addition of fissionable elements such as Uranium and Thorium compounds.

For the experiments described below it was necessary to have a γ-ray insensitive counter with as high a neutron efficiency as possible. Several attempts were made to incorporate Zns powder in a solid plastic material. Lucite chips were dissolved in acetic acid or in ethyl acetate and Zns powder was mixed in. However, the method was not successful, because when the plastic solution was too dilute the Zns powder settled out before hardening took place, and when the solution was less dilute it was difficult to introduce the Zns without also introducing air bubbles which destroyed the transparency. A compromise method has been developed using a large number of thin layers of Zns powder sandwiched between thin lucite plates, the whole assembly forming a rectangular block, from which the light produced in the Zns powder escapes through the plates into the photomultiplier.

Zinc sulfide activated with silver has a very high light conversion efficiency ranging from 20 to 28%. The emission spectrum is between 4000 and 6000 Angstroms with peaks at 4500 and 5200 Angstroms. The multiple crystalline powders are opaque for thicknesses greater than about 25 mg / cm^2. Grave and Dyson (1949) found that with 5 Mev α-particles the counting rate remains constant from 10 to 22 mg/cm^2 and beyond this thickness the counting rate falls rapidly. For these thicknesses the response to γ-radiation and high energy electrons is relatively small and the γ-ray pulses can be biased out electronically. Layers of equal thickness of Patterson D and R C A 33-Z-20 A ZnS phosphors were placed on the end of a photomultiplier with a lucite plate in front, and were tested with neutrons from a Ra-Be source. It was found that the R C A 33-Z-20 A powder gave about 30% more counts above the selected bias level and so this phosphor has been used throughout the following work.

The preliminary work was performed with an R C A 5819 photomultiplier. This tube has a cathode sensitivity of about 40 μa per lumen with a minimum limit of 20 μa per lumen. Its semi-transparent photocathode is deposited on the inner surface of the top of the tube

FAST NEUTRON COUNTER

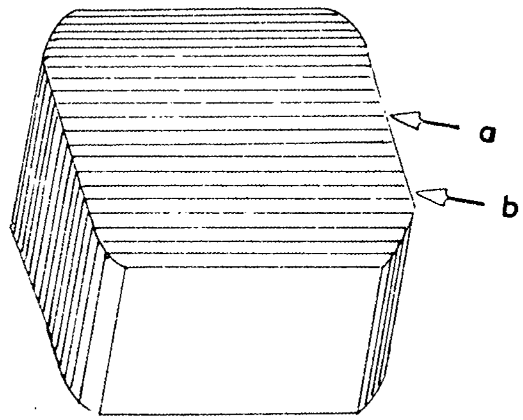

SANDWICH

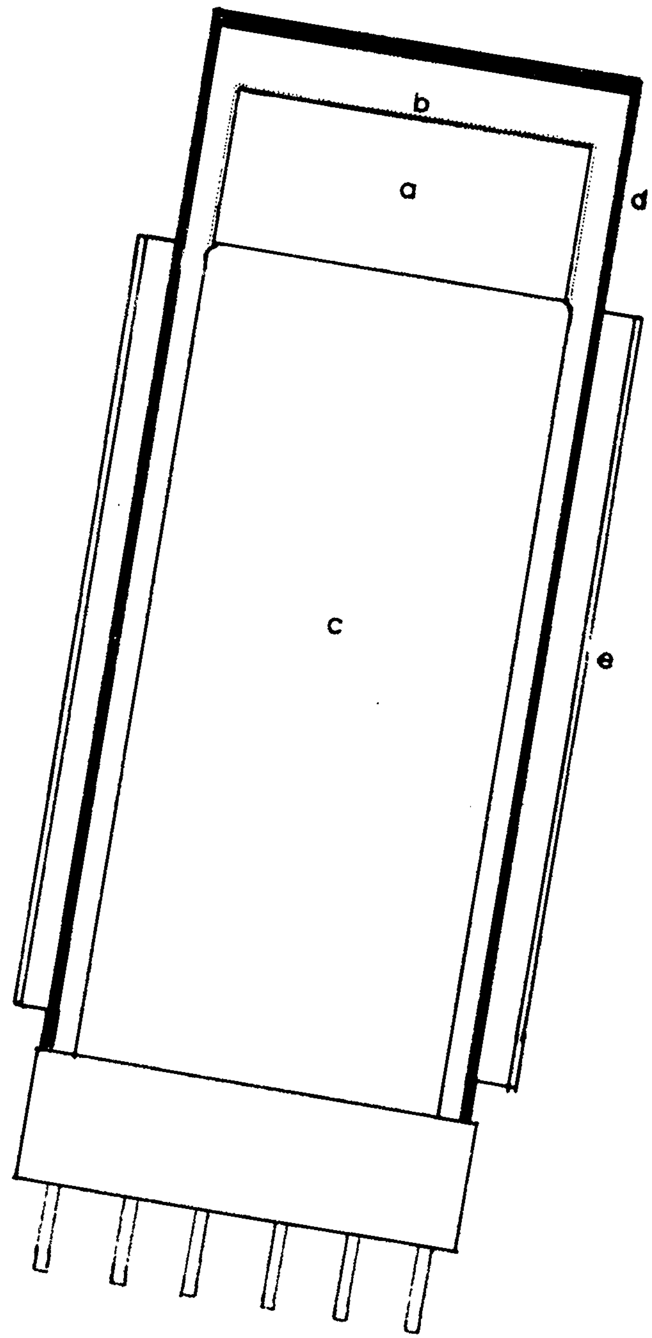

Fig. 1

Left Figure

a. ZnS powder - thin layer

b. Lucite light guide

Right Figure

a. ZnS - Lucite sandwich

b. MgO powder

c. Photomultiplier

d. Light cover

e. Magnetic shield

for good light collection. The spectral response extends from about 3000 to 6500 angstroms with a maximum at about 5000 angstroms which overlaps well with the emission spectrum of Zns. The final runs were made using a Dumont 6292 photomultiplier which has a spectral response from about 3100 to 6750 anstroms, with maximum sensitivity at about 4780 angstroms. The cathode sensitivity, between 40 and 60 μa per lumen, is greater than that of the R C A 5819 and also it has flat photocathode which facilitates the mounting of the phosphor.

Fig. 1 shows the construction and the mounting of the ZnS-plastic multiple sandwich. Thin lucite plates were dipped in ethyl formate and while still wet a weighed quantity of ZnS powder was sprinkled on evenly through a fine mesh nylon cloth. Then the plates were stuck together under pressure until dry. The block was polished on a face perpendicular to the plane of the plates. And this face was stuck to the photomultiplier with DOW-Corning 200 silicone oil which has a viscosity of 10^6 centistokes. Tests were made to determine the optimum thickness of the ZnS between the lucite plates. For thicknesses greater than 12 mg/cm^2 the γ-ray sensitivity becomes appreciable and thicknesses less than 10 mg/cm^2 gave a satisfactory neutron response. Several thicknesses of lucite plates were also tried and it was found that for Ra-Be neutrons the efficiency decreased for thicknesses greater than 0.125 inch. The optimum thickness depends of course on the neutron energy. The ranges of protons in lucite as calculated from their air ranges (Bethe and Livingstone 1937) are shown below:

Ep Mev	Range in air (cm)	Range in lucite (mm)
1	2.3	.025
2	7.1	.078
4	23.0	.25
6	46.7	.51
8	77.2	.85
10	110	1.2

The maximum thickness that can be used satisfactorily depends on the height of the block required, that is on the desirable total efficiency since, for a given height, if the plates are too thin, light is not transmitted from the top of the block to the photomultiplier. A check was made on the transmission of light down the block by preparing a Zns plastic sandwich with 0.125 inch thick lucite plates 5 inches long. This was placed endwise on the photomultiplier, a Ra-Be neutron source was placed 25 cm away to one side and the counting rate was observed, as a function

FAST NEUTRON COUNTER ELECTRONICS

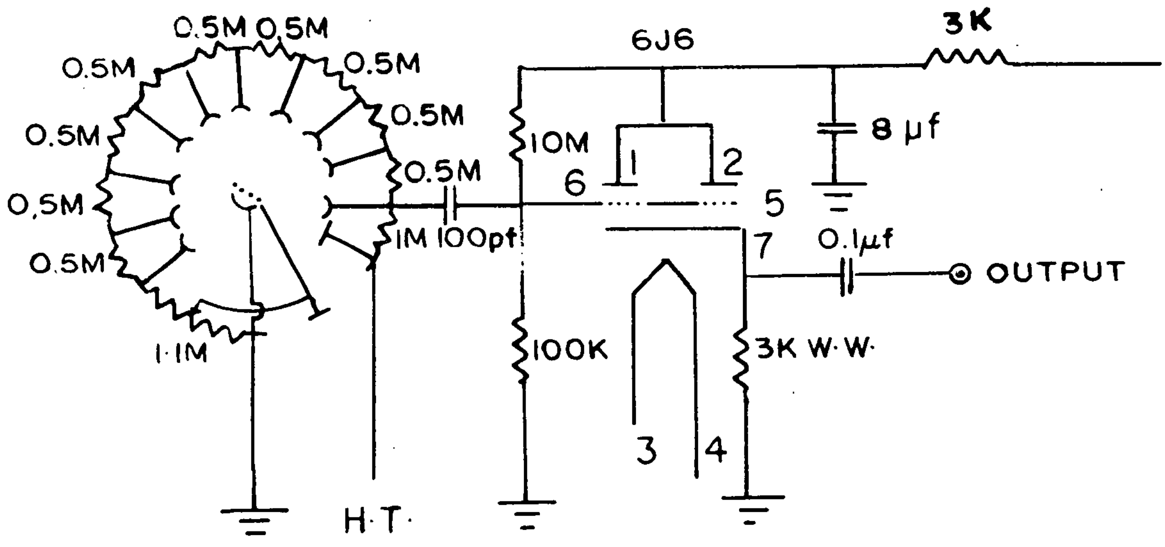

Dumont 6292 preamplifier

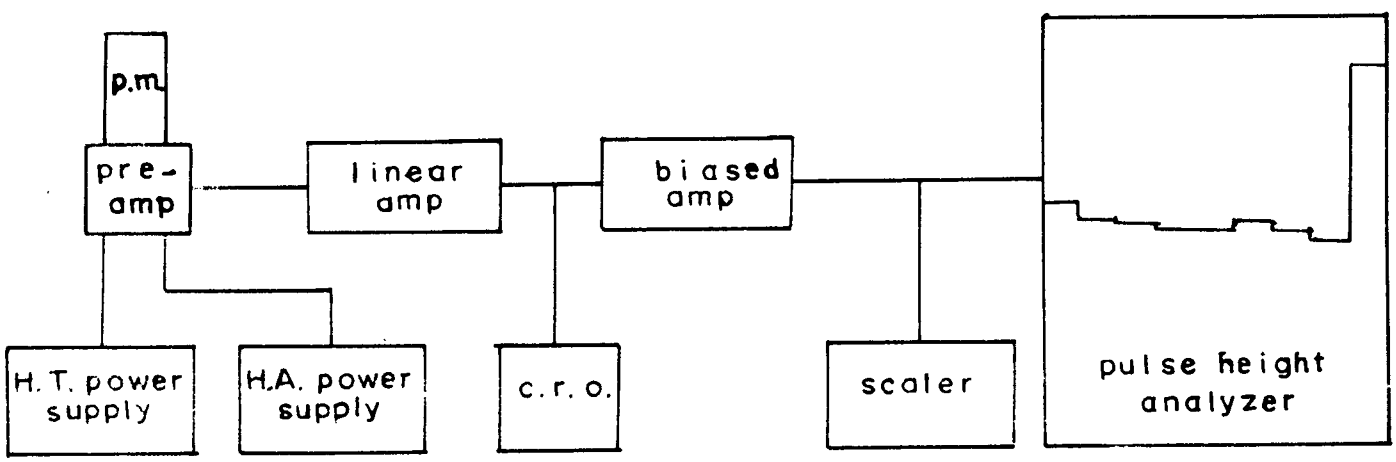

Fig. 2

of the length, which was altered by cutting sections from the end of the sandwich remote from the photomultiplier. It was found that there was little change in counting rate until the length was reduced below 3 inches and the counting rate became roughly proportional to the length for a length less than 1.5 inches.

Of the sandwich assemblies which were made for testing, details of two which had useful characteristics are given below:

	sandwich (1)	Sandwich (2)
lucite thickness	$\frac{1''}{32}$	$\frac{1''}{16}$
length	1 cm	2 cm
width	4.2 cm	4.4 cm
number of layers	50	23
thickness of Zns	7 mg/cm^2	7 mg/cm^2

Sandwich number one with the thiner plates had an efficiency $1\frac{3}{4}$ times that of number two. However, due to its smaller height it gave fewer counts for a given source strength than number two. Due to the light loss in the thin plates it was not desirable in this case to make the plates any higher. Sandwich number two was used for the measurements described below.

After the sandwich assembly was polished and stuck to the photomultiplier with DC 200 silicone oil it was covered with MgO powder produced by burning magnesium ribbon close to the surfaces. Finally a

Fig. 3

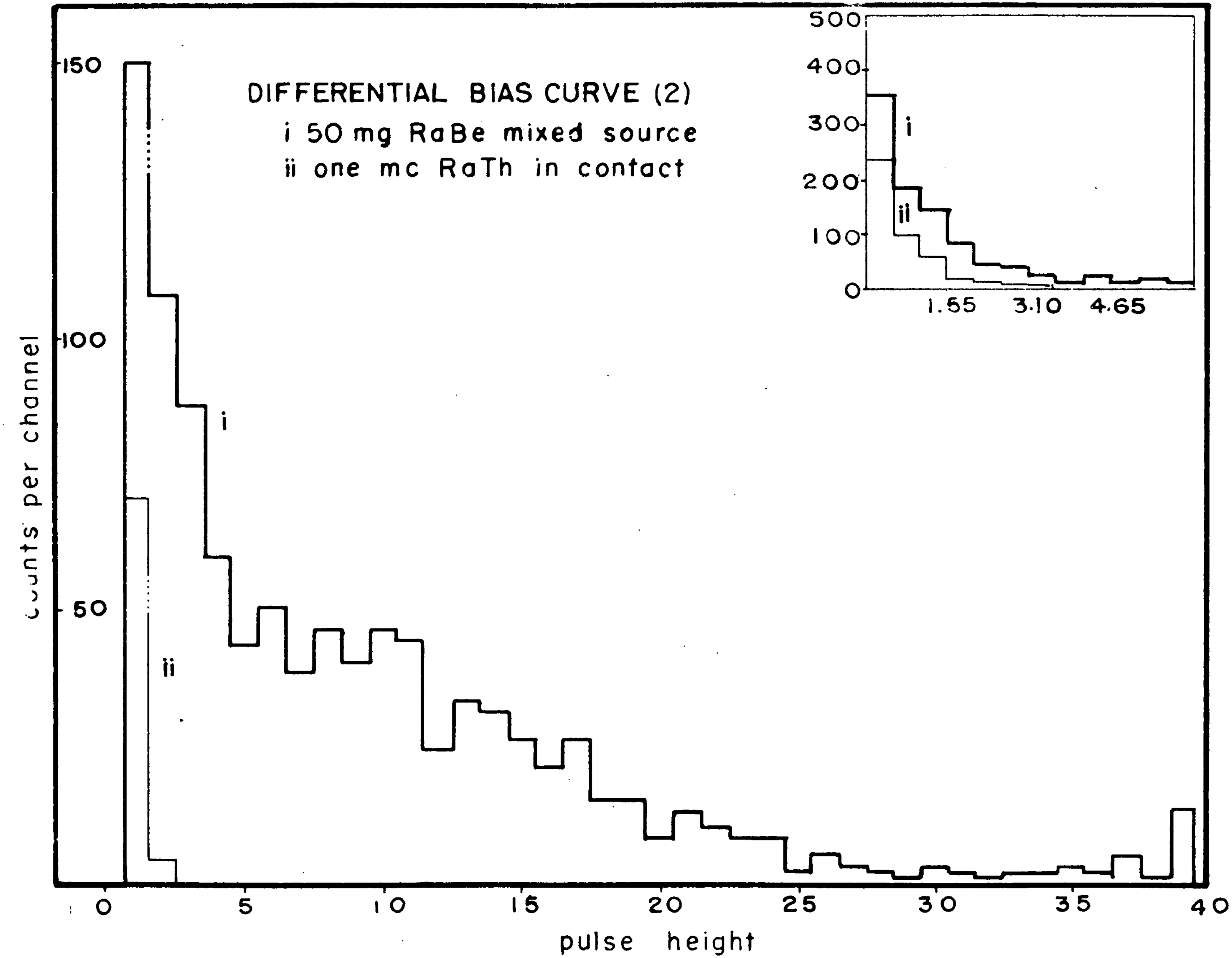
DIFFERENTIAL BIAS CURVE (2)
i 50 mg RaBe mixed source
ii one mc RaTh in contact
counts per channel
pulse height
150
100
50
0
5
10
15
20
25
30
35
40
i
ii
500
400
300
200
100
0
1.55
3.10
4.65

Fig. 3

Fig. 4

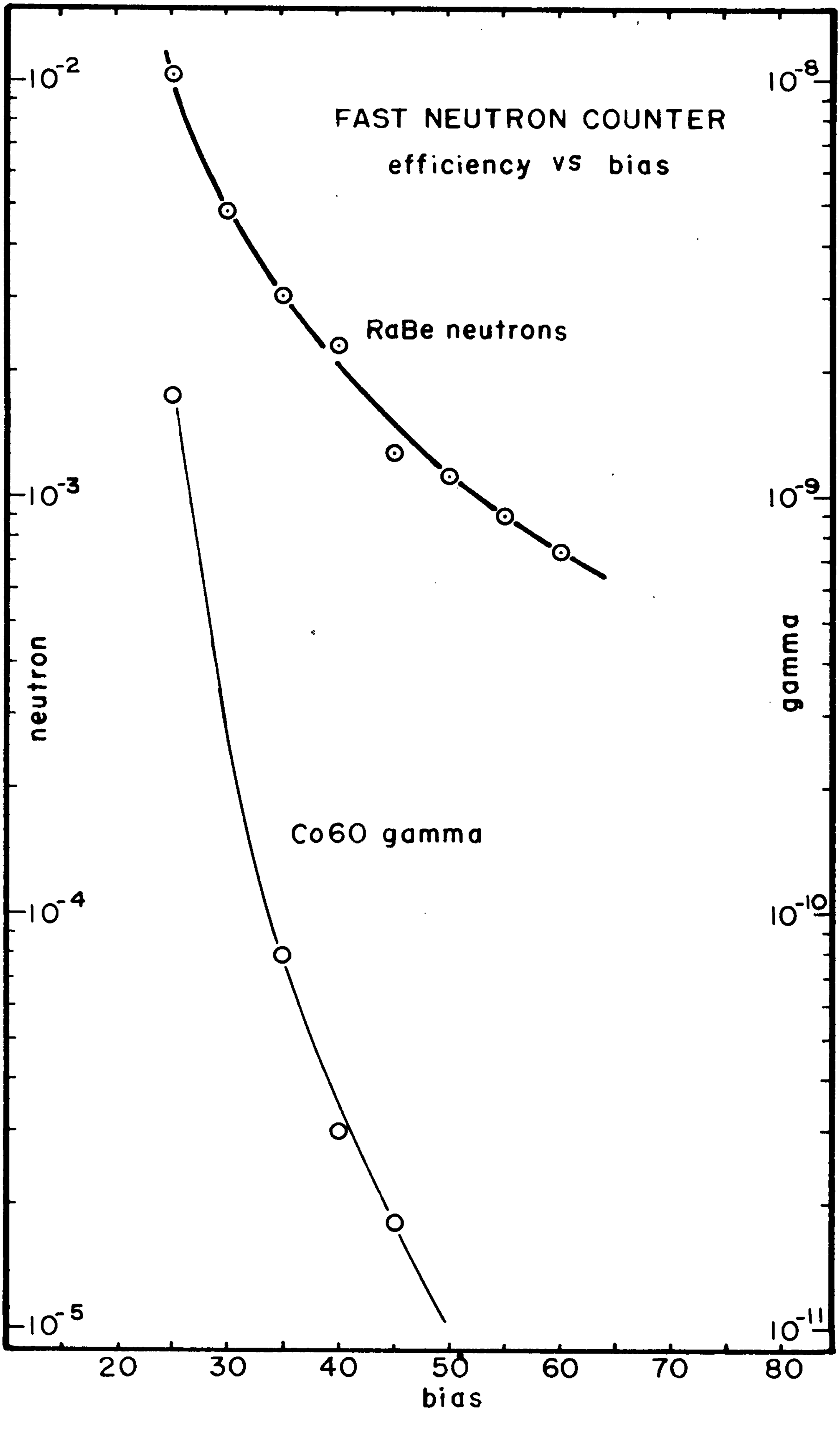

FAST NEUTRON COUNTER
efficiency vs bias
RaBe neutrons
Co60 gamma
neutron
gamma
10^{-2}
10^{-3}
10^{-4}
10^{-5}
10^{-8}
10^{-9}
10^{-10}
10^{-11}
20
30
40
50
60
70
80
bias

brass light shield was placed over the phosphor and the photomultiplier and a magnetic shield put in position as shown in figure 1). The arrangement of the preamplifier and the subsequent electronics are shown in Fig. 2. The photomultiplier was operated at 1250 volts from a well-stabilized powder pack. The signal output after passing through the preamplifier cathode follower was amplified by a Northern Electric type 1444 linear amplifier. The pulses were finally passed via a biased amplifier to a scaler and to the 30 channel "Canadian Marconi" kicksorter.

Counter performance

Fig. 3 shows a bias curve for the fast neutron multiple sandwich counter when a 50 mg Ra-Be source was placed 25 cms from the sandwich. Also shown is the spectrum produced by a one millicurie RaTh γ-ray source in contact with the counter. A comparison between the neutron and gamma ray sensitivities was made using Ra-Be and Co^{60} sources of known strengths. The results as a function of discrimination bias are shown in Fig. 4.

It is clearly apparent that a reasonable neutron efficiency can be obtained at bias levels for which the gamma-ray sensitivity and the counter background are very low indeed.

Fig. 5

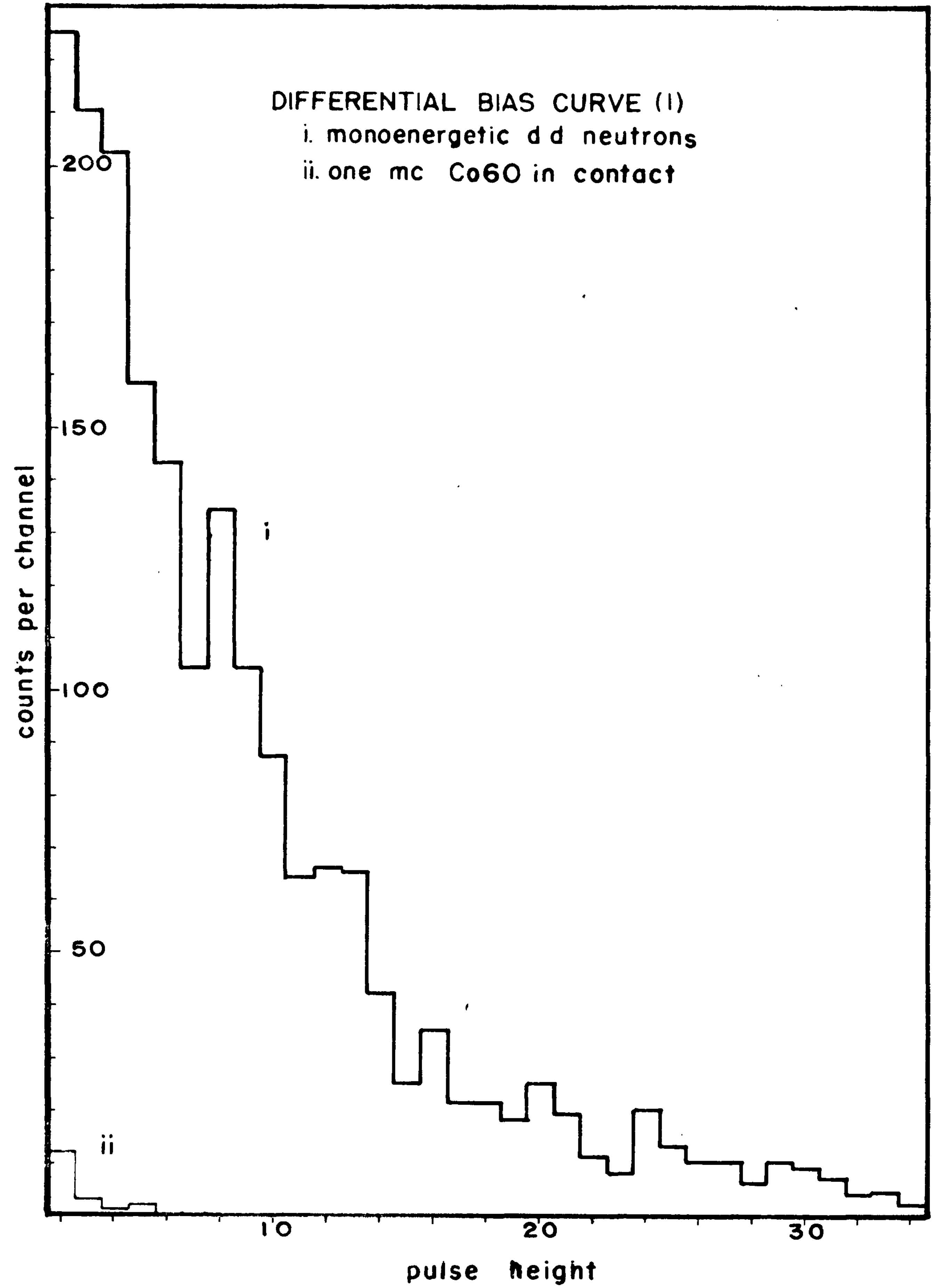
DIFFERENTIAL BIAS CURVE (I)
i. monoenergetic d d neutrons
ii. one mc Co60 in contact
i
ii
200
150
100
50
10
20
30
counts per channel
pulse height

Fig. 5a

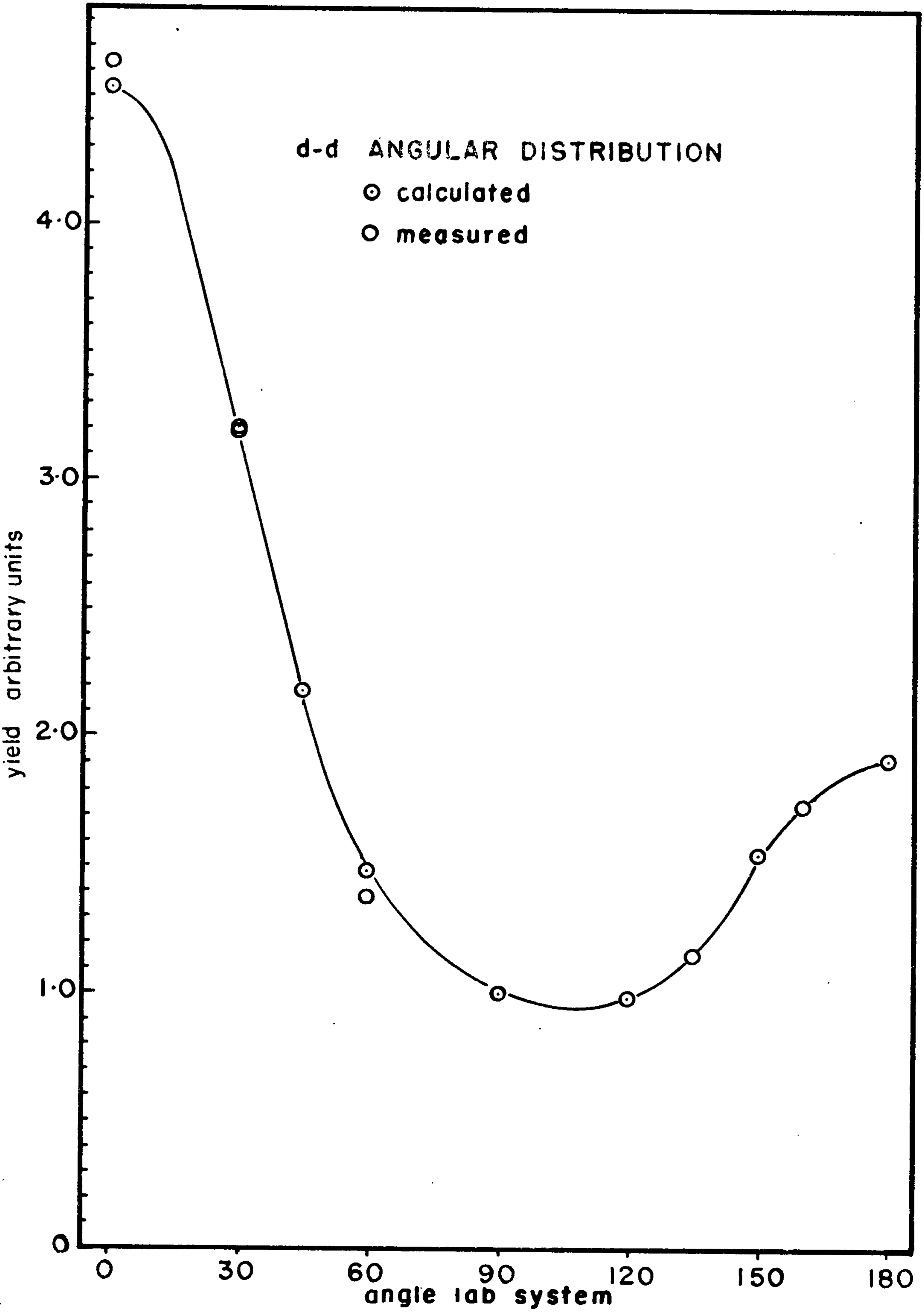
d-d ANGULAR DISTRIBUTION
⊙ calculated
O measured
4·0
3·0
2·0
1·0
0
yield arbitrary units
0
30
60
90
120
150
180
angle lab system

Fig. 5 shows the spectrum obtained with d on d neutrons produced by the U.B.C. 50 Kev accelerator. For a bias at which the counter had negligible response to RaTh gamma rays the efficiency for 4.3 Mev d on d neutrons (produced by the U.B.C. Van de Graaff generator) was 0.77%. Under these conditions only four counts were recorded when the counter was placed 40 cms. from a flourine target which was bombarded for 8 minutes with 650 millicoulombs of protons covering the 873 fluorine resonance. The cosmic ray and local background under these conditions is only five or six counts per hour. The angular distribution of the d on d neutrons, produced by bombarding a thin D_2O target with one Mev deuterons, was measured and the experimental results were compared with the angular distribution which was calculated from results given by Hunter and Richards (1947). These workers measured the d on d neutron angular distribution at several energies with a BF_3 counter and from their results have given an expression for the angular distribution as a function of deuteron energy. The measured and calculated values are shown in Fig. 5a. The agreement between the two sets of data is very satisfactory indicating that the efficiency of the multiple-sandwich for neutrons from two to four Mev is quite independent of neutron energy.

Fig. 6

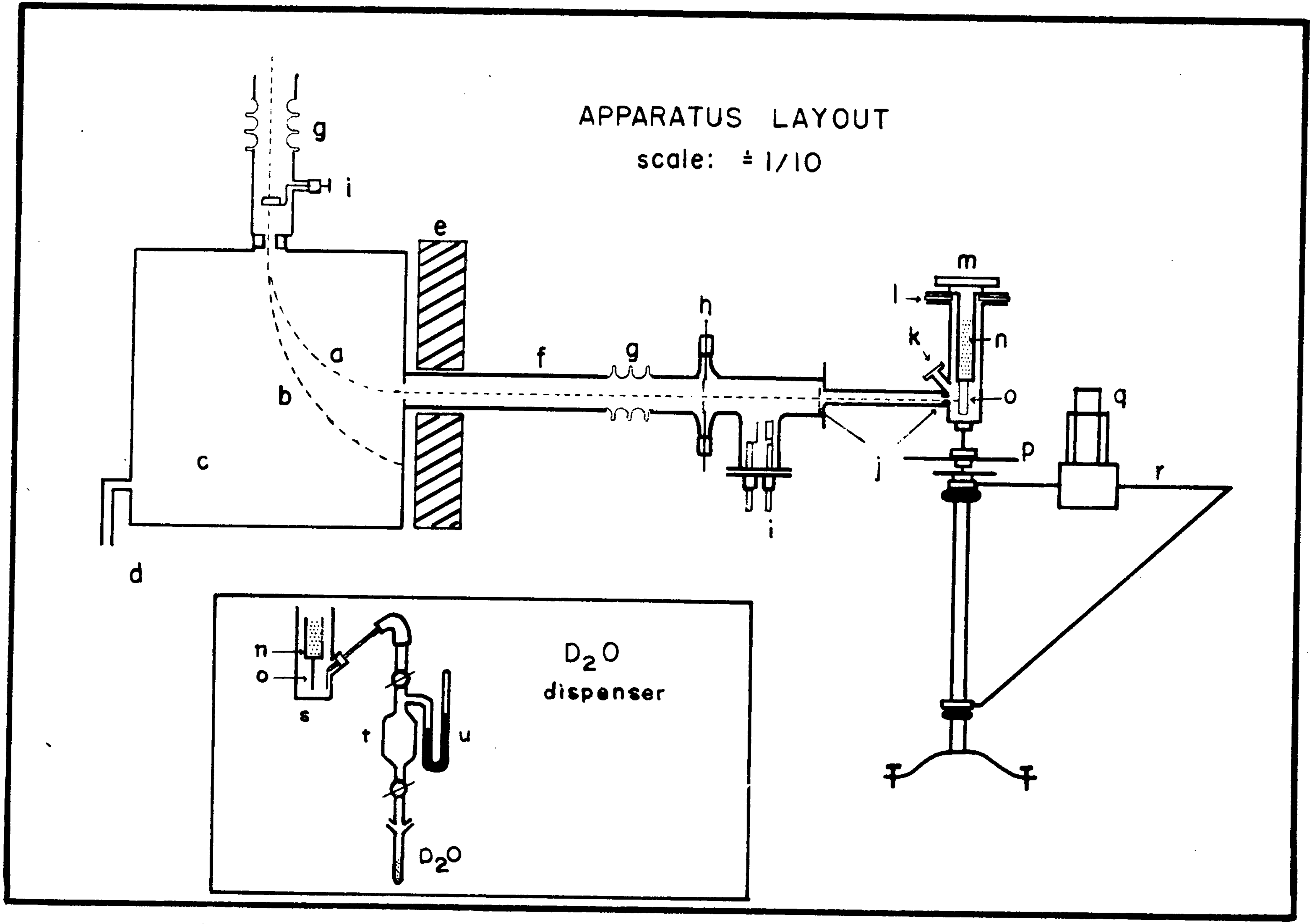
APPARATUS LAYOUT
scale: ≐ 1/10
a
b
c
d
e
f
g
h
i
j
k
l
m
n
o
p
q
r
n
o
s
t
u
D_2O
dispenser
D_2O

a. proton beam

b. mass two beam

c. magnet box (size not in proportion)

d. pumping outlet

e. paraffin shield

f. glass tube

g. bellows

h. beam stabilizing slits

i. quartz focussing plate

j. tungsten stops

k. window

l. lucite insulating disc

m. liquid air trap

n. liquid air

o. gold target backing

p. degree circle

q. fast neutron counter

r. rotating arm

s. nickel tube

t. 50 cc bulb

u. Hg manometer

Chapter III

NEUTRON MEASUREMENTS

1. Apparatus

The target was supported on a copper plate suspended from the bottom of a liquid air trap. Heavy water vapor was frozen on a gold plate 1.5 mm thick, which was screwed to the copper plate. The gold plate was thoroughly cleaned as follows. After successive rinses of concentrated sulfuric acid and sodium hydroxide solution the plate was washed with distilled water and pure alcohol and electrically etched in potassium cynide solution for eight hours until crystal structure was apparent on the surface. Finally it was rinsed with distilled water and baked for a few hours at 100°C. Measured volumes of D_2O vapor from the dispenser could be admitted to the target chamber via a small hole in a nickel tube facing the target. The target chamber was supported on a stand provided with a degree circle for measuring the angular position of the neutron counter which was mounted on a rotatable arm as shown in Fig. 6. Prior to final assembly the target chamber and its vacuum connections were baked to

Fig. 7

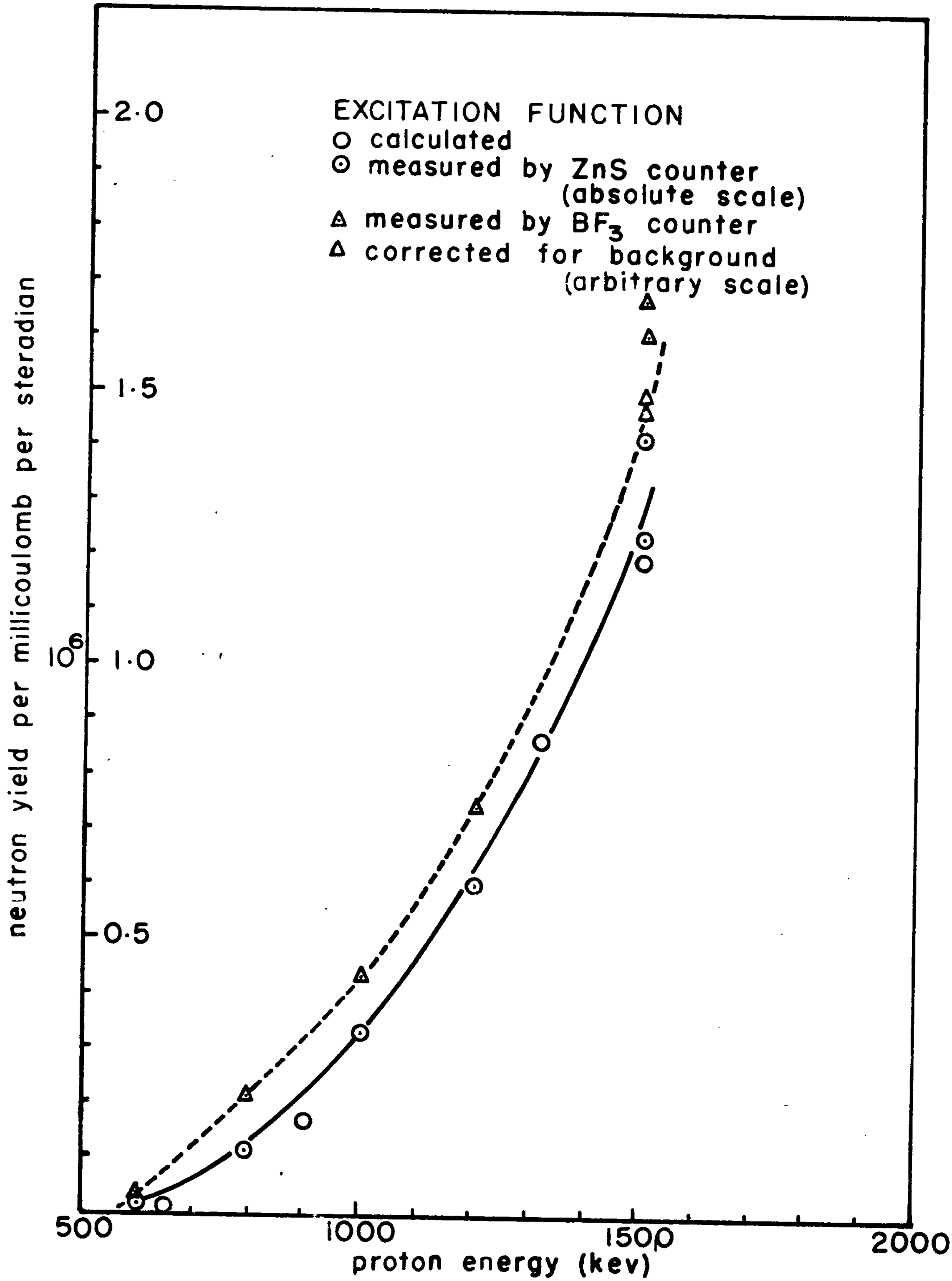

2·0
1·5
10^6 1·0
0·5
EXCITATION FUNCTION
o calculated
⊙ measured by ZnS counter
(absolute scale)
Δ measured by BF_3 counter
Δ corrected for background
(arbitrary scale)
neutron yield per millicoulomb per steradian
500
1000
1500
2000
proton energy (kev)

remove all traces of water and organic vapors which could have formed a contaminating deposit when the target was cold. On the backside of the copper target mounting plate there was a thin CaF_2 target evaporated on a tungsten backing. This was used to measure target thicknesses as described below. The target and the liquid air trap were insulated from the outer target chamber and maintained at a potential of +300 volts with respect to the rest of the apparatus in order to suppress the secondary electron emission. Tungsten stops were used to define the beam hitting the target. The integrated current falling on the target was measured by an electronic integrator (Edwards 1951).

2. Measurements

The measurements can be divided into five parts which will be described separately.

(a) Excitation function for neutron production

The 0° neutron yield from a thick D_2O ice target has been measured for proton bombarding energies of 1500, 1200, 1000, 800 and 600 Kev. using the BF_3 long counter and the ZnS lucite sandwich fast neutron counter described above. The results obtained are shown in Fig. 7; it can be seen that the neutron yield increases rapidly with increasing proton energy. Also shown, by the open circles, are points representing the neutron yield as calculated from the theory for the double process described below.

The yield as measured by the BF_3 long counter is indicated by triangles; the vertical scale of this curve is arbitary since it was difficult to define the solid angle, when the front of the counter was only one third of the counter length from the target. The 1500 Kev points have had 15 percent background subtracted. The background presumably arose due to the sensitivity of the BF_3 counter to the low-energy degraded neutrons initially produced by the mass-two beam in the magnet box. The background was measured by interrupting the proton beam by the quartz plate as described in detail in section "d". It is worth noting that the background in the Zns plastic sandwich counter was negligible during the excitation function runs.

(b) Target thickness calibration

In order to measure the absolute yield of neutrons from a thin target it was necessary to know the number of deuterons per square cm. on the target. This was determined in the following manner. The target was rotated to expose the CaF_2 to the proton beam and an excitation curve was obtained for the 873 Kev resonance of the $F^{19}(p,\alpha,\gamma)$ reaction by observing the γ-rays in a NaI scintillation counter. Then the target was turned to face the nickel tube from the D_2O vapour dispenser and after the target was cooled

Fig. 8

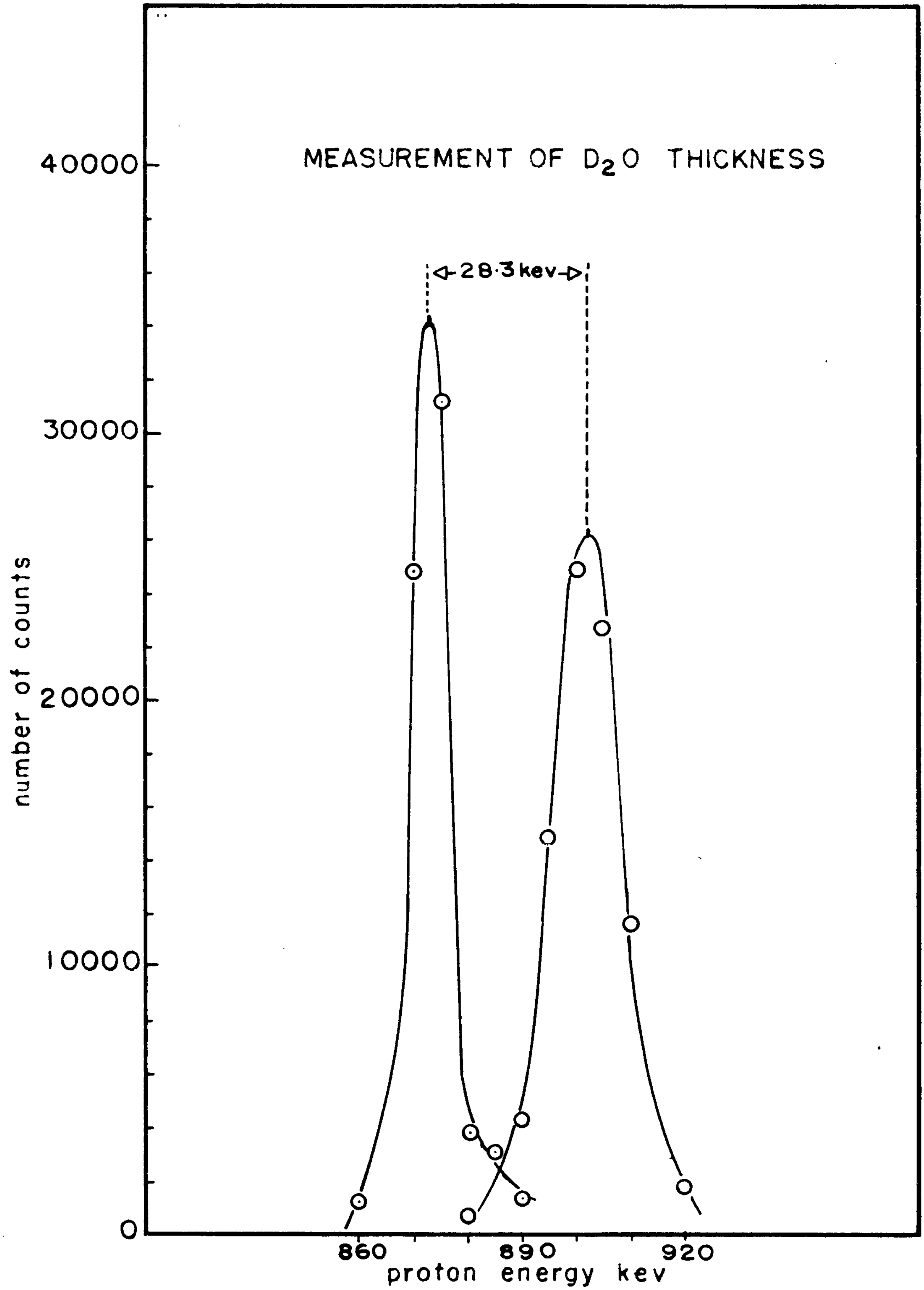
MEASUREMENT OF D_2O THICKNESS
28·3 kev
40000
30000
20000
10000
0
number of counts
860
890
920
proton energy kev

with liquid air, a standard quantity of D_2O vapor, hereafter called one scoop, was admitted to the target chamber where it froze on top of the CaF_2. Finally the CaF_2 was turned back to face the proton beam and a second excitation curve was obtained for the 873 Kev resonance. In this case the resonance occurs for proton energies higher than 873 Kev. by an amount equal to the loss of proton energy in passing through the D_2O ice layer as shown in Fig. 8. From the measured shift in resonance energy and from a knowledge of the stopping power of ice for protons, the thickness of the ice layer can be obtained. The stopping power of heavy ice has been carefully measured for protons in the range 18 to 540 Kev by Wenzel and Whaling (1952). In this energy range the agreement with Bethe's theory is good and so some confidence can be placed in values of the stopping power calculated by Hirschfelder and Magee (1948) using the same theory but for higher proton energies. Therefore once the shift in resonance energy E has been measured the target thickness Δx can be calculated. For a target consisting of one standardized scoop of D_2O vapor, the shift in the 873 Kev resonance was found to be 28.3 ± 5 Kev as shown in Fig. 8. From the values of ΔE versus Δx obtained from the above theory, and tabulated by Griffiths (1953) it can be shown that a ΔE of 28.3 Kev for protons of 890 Kev corresponds to a target thickness of 1.18×10^{-4} cm. In this way a calibration of the target thickness per scoop was obtained. In subsequent work it has been assumed that a target laid down under exactly the same conditions as the calibration target had the same thickness per scoop. Also it has been assumed that for targets thicker than one scoop the thickness was proportional to the number of scoops.

In order to make thick targets both valves of the dispenser were opened for seven minutes and the neutron yield under proton bombardment was measured. Then the valves were opened for a further seven minutes and the neutron yield was measured again. This process was repeated three times, until there was no further increase in neutron yield. Finally the valves were opened for a further four minutes to make absolutely certain that the target was "thick", i.e. at the particular bombarding energy all incident-protons and scattered deuterons were stopped in the ice layer.

Fig. 9

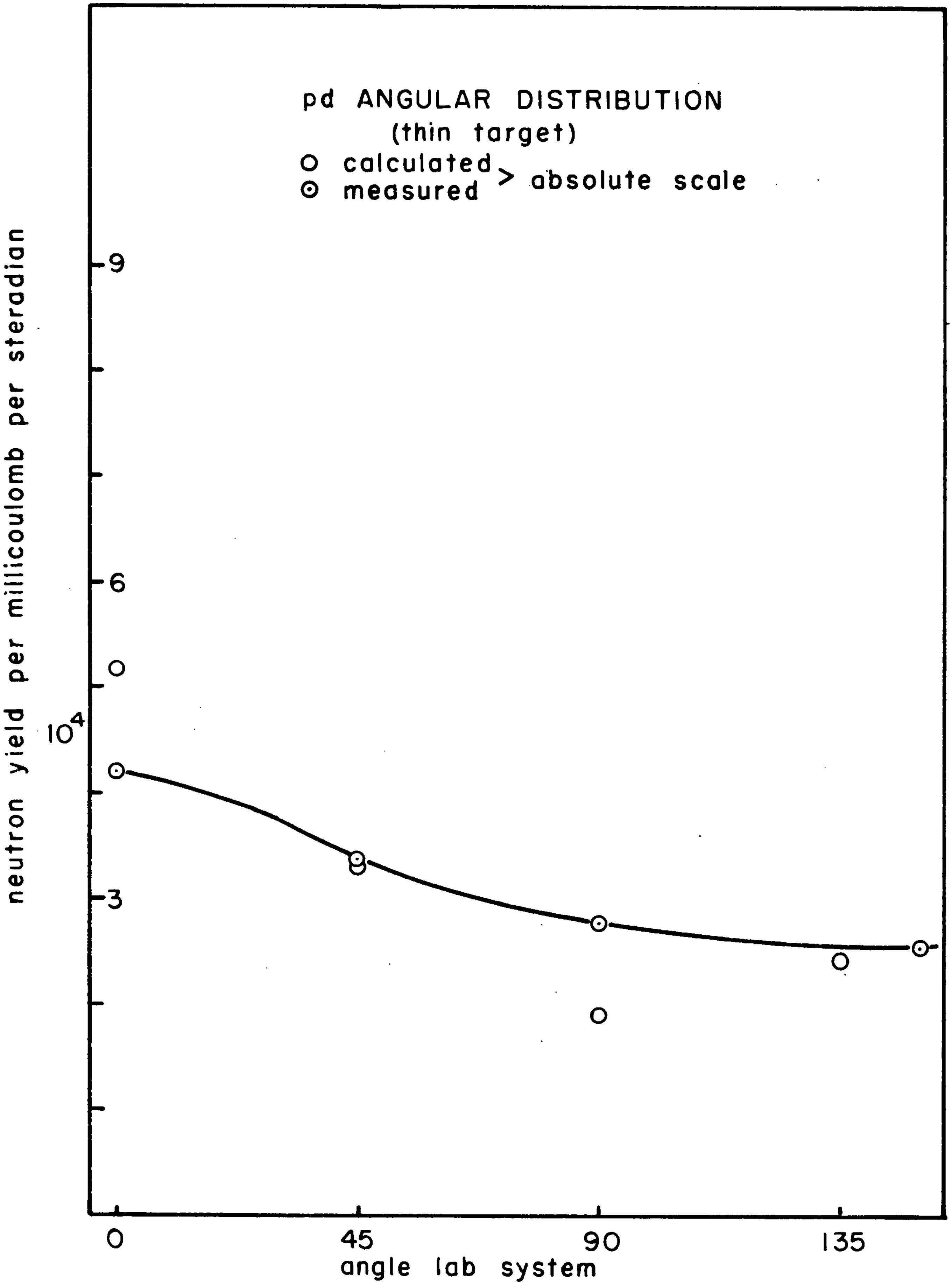

pd ANGULAR DISTRIBUTION
(thin target)
calculated
measured
absolute scale
neutron yield per millicoulomb per steradian
9
6
10^4
3
0
45
90
135
angle lab system

(c) <u>Thin target yield and angular distribution</u>

A thin target consisting of three scoops of D_2O vapor was set at 45° to the incident beam and was bombarded with 1.5 Mev protons. The reaction was monitored with a NaI scintillation counter set at 90° to the incident proton beam in order to count the gamma rays from the $D(p,\gamma)He^3$ process, and the neutron yield was measured with the fast neutron scintillation counter as a function of the angle of the counter with respect to the incident beam direction. Measurements of the incident beam current, the number of neutron counts and the number of gamma ray counts, were made with the fast neutron counter at 0°, 45°, 90°, and 150°. The results after taking into account the efficiency and solid angle of the neutron counter are given in the table below. The errors quoted are statistical errors only. No correction has been made for neutron absorption by the target backing. The counter was placed 8.3 cms. from the target. Also shown in the table are figures for the yield on the basis of the double process obtained from calculations given below. Fig. 9 shows the results graphically.

<u>Neutron yield per steradian</u>

<u>per millicoulomb of proton beam</u>

Detector position	0°	45°	90°	135°	150°
measured	42200	33800	27900		25500
	±4.7%	±5.1%	±5.7%		±5.7%
calculated	51700	33200	19100	24500	

Fig. 10

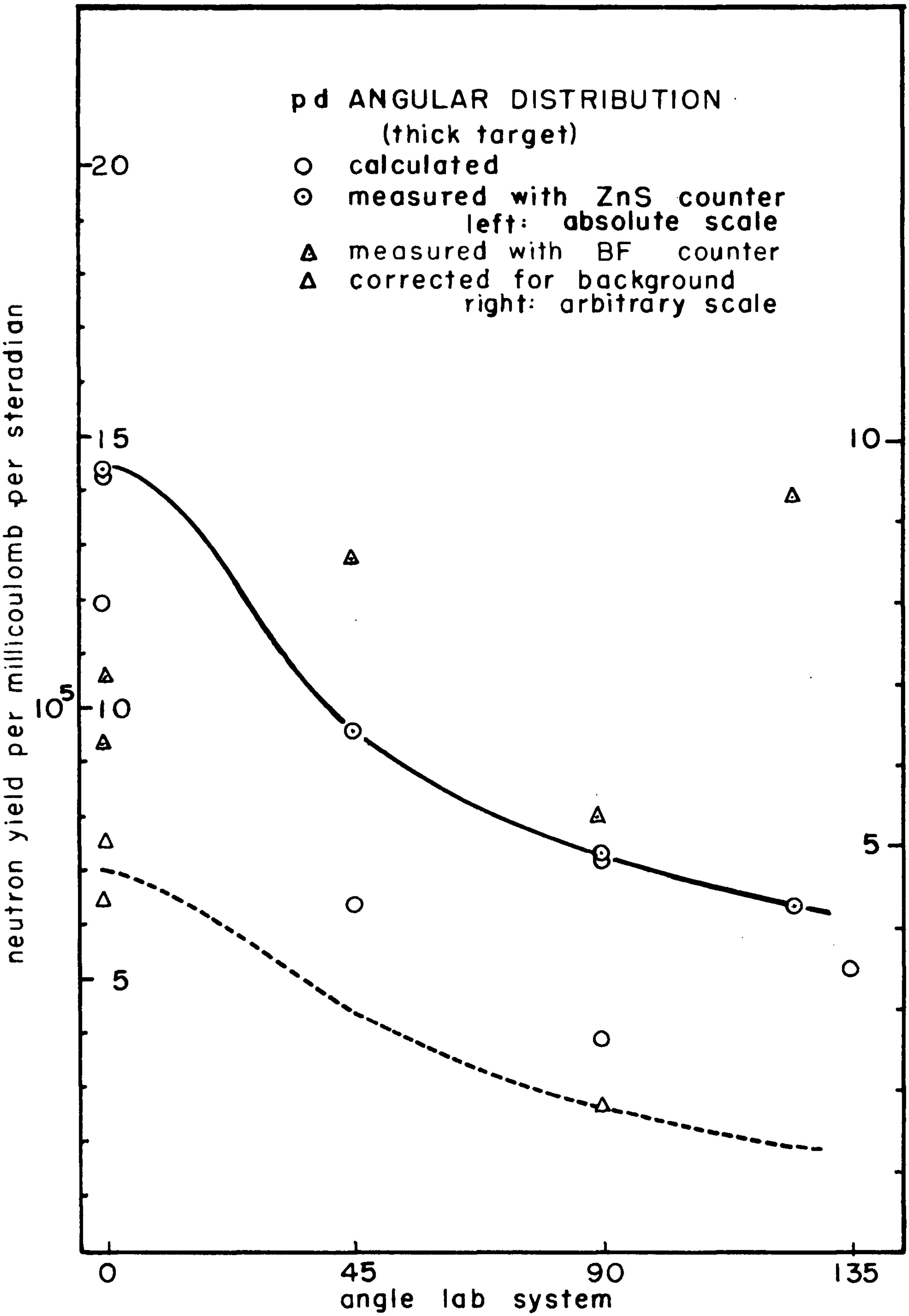

pd ANGULAR DISTRIBUTION
(thick target)
calculated
measured with ZnS counter
left: absolute scale
measured with BF counter
corrected for background
right: arbitrary scale
neutron yield per millicoulomb per steradian
20
15
10^5 10
5
10
5
0
45
90
135
angle lab system

(d) Thick target yield and angular distribution

A thick target was laid down, and placed perpendicular to the proton beam. The neutron yield was measured at 0°, 45°, 90°, and 125°, for a proton bombarding energy of 1.5 Mev. A NaI scintillation counter served as a monitor by counting the $D(p,\gamma)He^3$ gamma rays. The fast neutron counter was placed 10.7 cms., center to center, from the target. The final results are given in Fig. 10 and in the table below in terms of the neutron yield per steradian per millicoulomb of protons obtained after taking into account the neutron counter efficiency and solid angle.

Neutron yield per steradian

per millicoulomb of proton beam

Detector position	0°	45°	90°	125°	135°
measured	14.4×10^6	9.57×10^6	7.3×10^6	6.32×10^6	
	±2.8%	±3.5%	±7.2%	±4.0%	
calculated	11.9×10^6	6.36×10^6	3.87×10^6		5.12×10^6

The last line indicates the calculated yield. Also shown are the statistical counting errors.

Since the neutron yield from the thick target was considerably greater than that from the thin target, it was also possible to use the BF_3 counter in these measurements. The front of the BF_3 counter was placed 33.9 cms. from the target at 0°, 45°, 90° and 125°, and the number of counts observed at each angle is shown in the following table.

counter position	0°	45°	90°	125°
number of neutron counts	6700	8560	5370	9300
number of gamma ray counts	46100	46800	44700	47000
neutron background counts	1970		3630	
corrected neutron counts	4730		1740	

The angle distribution indicated by the uncorrected BF_3 counter results is much more isotropic than that for the fast neutron counter given above. The BF_3 counter is, however, sensitive to the rather large background of slow neutrons. A separate background run was made at 0° and 90° with the proton beam interrupted by the quartz focussing plate, with the results shown in the table. The final line in the table indicates the BF_3 counter results at 0° and 90° after correction for the background, and it is apparent that the angular distribution obtained in this way is in rough agreement with the fast neutron counter results as shown in Fig. 10. It was noted that the BF_3 counter background was greater, the closer the counter was to the magnet box.

Fig. 11

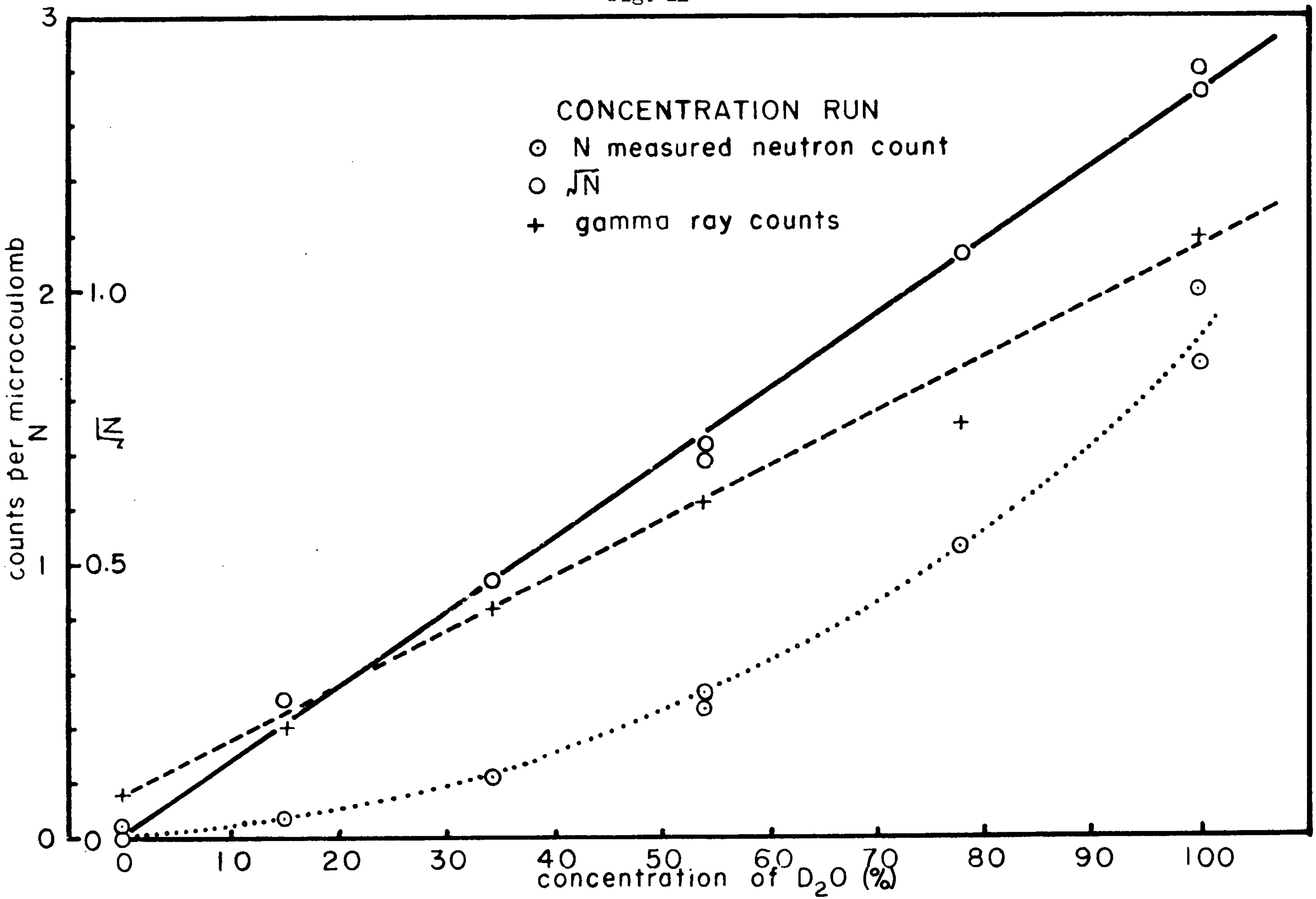

CONCENTRATION RUN
N measured neutron count
√N
gamma ray counts
counts per microcoulomb
N
√N
3
2
1
0
1.0
0.5
0
0
10
20
30
40
50
60
70
80
90
100
concentration of D_2O (%)

(e) Concentration run

In order to provide a further test of the double process hypothesis the neutron yield at 0° for 1.5 Mev protons was measured with thick D_2O + H_2O mixed targets, with percentages of D_2O ranging from 100 to 0 percent. The results are shown in Fig. 11. The gamma-ray yield is directly proportional to the deuteron concentration in the target as expected from the fact that the gamma rays arise from the direct $D(p,\gamma)He^3$ process. However, the square root of the neutron yield is proportional to the deuterium concentration, or in other words, the neutron yield is proportional to the square of the deuterium concentration. This experiment strongly supports the hypothesis of the double-process origin of the neutrons, as suggested in the introduction.

Fig. 12

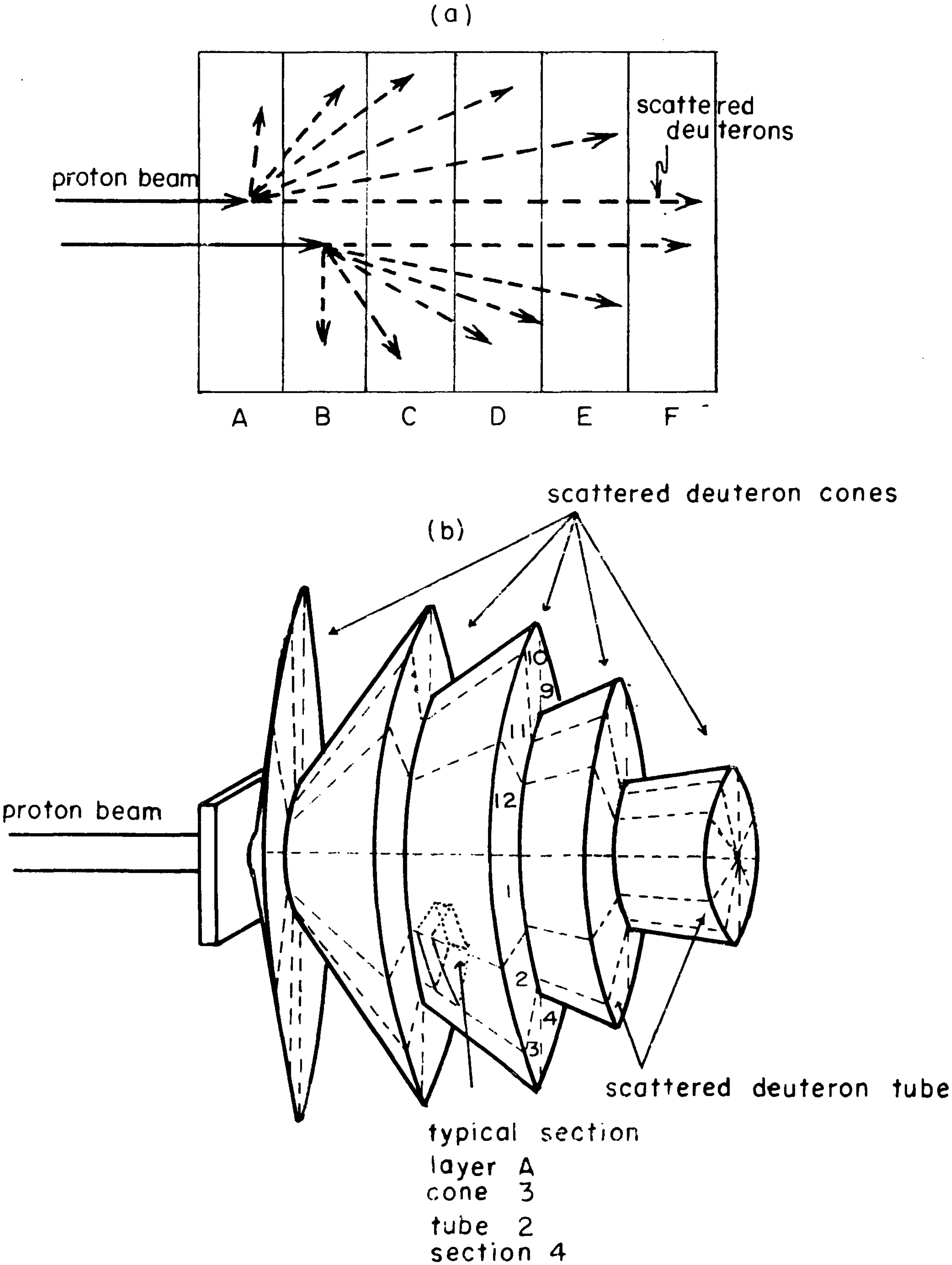
(a)
scattered
deuterons
proton beam
A
B
C
D
E
F
(b)
scattered deuteron cones
proton beam
10
9
11
12
1
2
4
3
scattered deuteron tube
typical section
layer A
cone 3
tube 2
section 4

Chapter IV

CALCULATIONS

1. Introduction

Calculations have been made of the yield, excitation function, and angular distribution, of neutrons from thick and thin targets of D_2O ice bombarded with protons, on the assumption that they are caused by the double process suggested above, i.e. deuterons scattered by incident protons cause subsequent $D(d,n)He^3$ neutrons by collision with further D atoms in the target.

2. Outline of Calculation Method

In the case of a thick target the calculations follow the physical processes step by step as follows. The target is divided into 6 layers perpendicular to the proton beam as shown in Fi. 12(a), and in each layer the protons are considered to have a constant energy equal to the mean energy of the actual protons while in the layer. From a knowledge of p-d scattering the energy and the angular distribution of the deuterons scattered from each layer is calculated. The scattered deuterons from any layer can be divided into overlapping cones symmetrical about the proton beam direction as shown in Fig. 12(b). It was assumed that all the deuterons in each cone had an initial energy equal to the mean initial energy of the deuterons in the cone, this energy being obtained by simple mechanics knowing the angle of the cone and the incident proton energy. Each cone was divided into 12 tubes running out from the apex and equally spaced about the cone axis. The angle between the axis of each tube and the line joining the target and the neutron counter was then obtained by geometrical methods, so that knowing the angular distribution of the neutrons emitted by $D(d,n)He^3$ reaction caused by deuterons travelling down the cone, through the heavy ice, it was possible to obtain the contribution from each tube in the direction of the detector. As the deuterons travel down each tube they lose energy and so the tubes were divided into sections along their length as shown in Fig. 12(b) and in each section the deuterons were assumed to have an energy equal to the mean deuteron energy in the section. The table below gives a rough idea of the number of subdivisions used in the calculation.

Subdivision	Number used
Layers	6 (A,B,C,D,E,F)
Cones	number depends on layer, e.g. 6 for layer A, 3 for layer D and 1 for layer F.
Tubes	12 for each cone
Tube sections	number depends on the particular layer and cone i.e. on deuteron

energy, e.g. 6 for layer A cone 1, 3 for layer A cone 4 and 3 for layer D cone 1.

Actually the total number of sections was 252 for layer A alone and 672 for all 6 layers. Finally from a knowledge of the energy and angular dependence of neutron yield for the $D(d,n)He^3$ reaction it was possible to calculate the contribution of each section to the neutron yield in the detector direction. After the individual section contributions were calculated, the total neutron yield in the counter direction can be obtained by summing over all sections of each tube, over all tubes of each cone, over all cones of each layer and over all layers. The process was repeated for 4 different counter positions namely 0°, 45°, 90° and 135° between the proton beam direction and the counter to target direction, to give the angular distribution shown in Fig. 10. Further details concerning the cross-section parameters employed in the calculation are given below.

3. Calculation Details

The target was divided into layers each one having approximately $\frac{1}{6}$ of the incident proton energy of 1.5 Mev dissipated in it. From the known stopping power of heavy ice for protons (Wenzel and Whaling 1952, Griffiths 1953) the corresponding thickness in cms. of each layer was obtained. The energy of the protons in each layer was assumed to be constant and equal to the average energy of the protons in the layer. Then the number and the angular distribution of deuterons scattered out of each layer was obtained as follows: The scattering cross-section of deuterons for incident protons has been measured at 1510 Kev and 825 Kev by Bailey et al (1947) and at 250 Kev by Taschek (1942). From the angular distribution and cross-section data of these authors angular distribution and cross-section curves were interpolated for the mean proton energies assumed for each layer. Thus, from these curves the number of deuterons scattered from any layer into any angle could be estimated. Also from the mechanics of the scattering process (Schiff) the energy of the deuterons from any layer at any angle could be obtained. The scattering is symmetrical about the proton beam direction. Therefore since the problem has to be numerically integrated the scattered deuterons were divided into cones; the angular limits of each cone were defined in terms of approximately equal energy intervals of the scattered deuterons, and it was assumed that these deuterons all have an energy equal to the mean energy of the deuterons in the cone. Since it would have been difficult to integrate the graphical results concerning the number and angular distribution of scattered deuterons given above over the angles of

Fig. 13

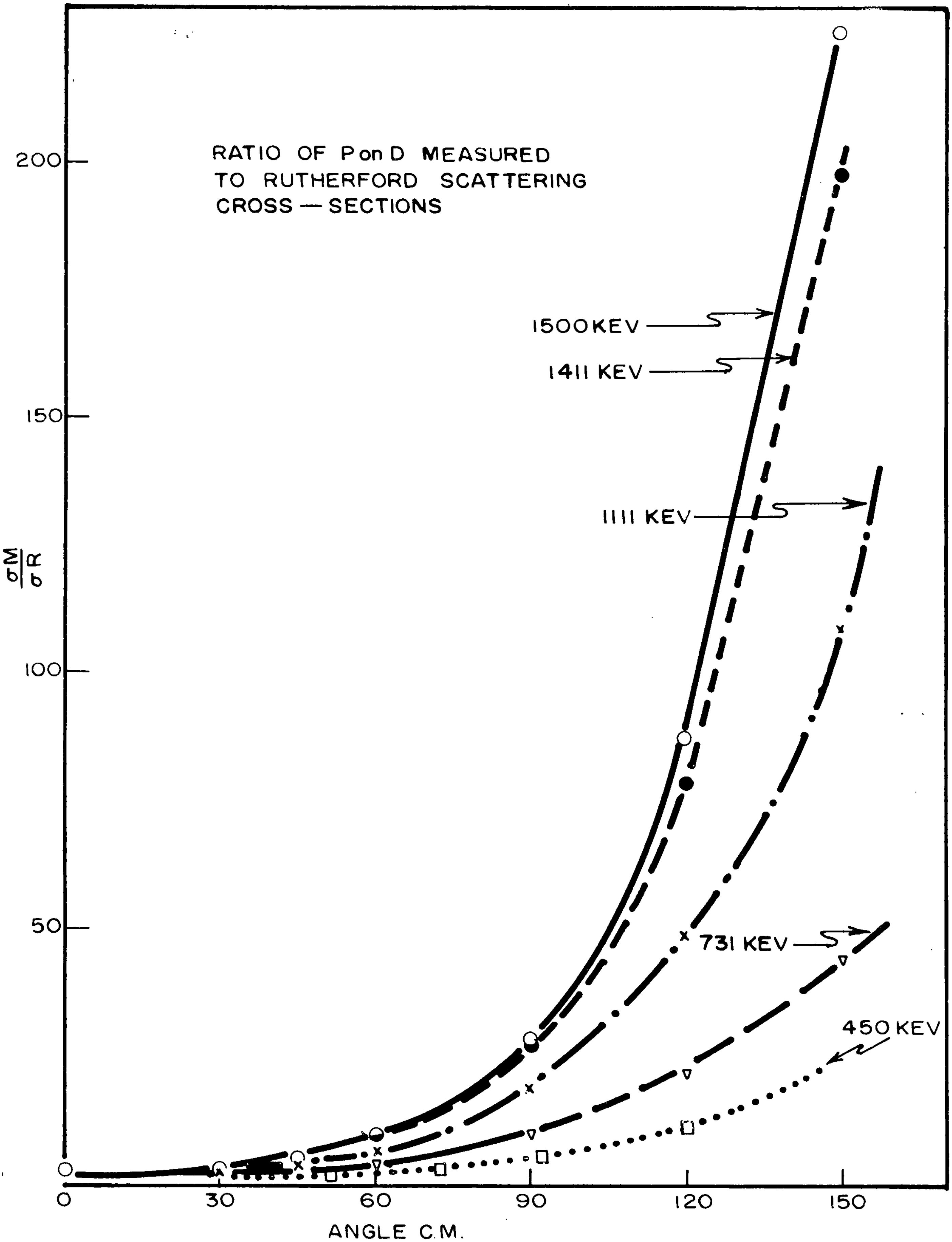
RATIO OF P on D MEASURED
TO RUTHERFORD SCATTERING
CROSS — SECTIONS
1500 KEV
1411 KEV
1111 KEV
731 KEV
450 KEV
200
150
100
50
0
30
60
90
120
150
ANGLE C.M.
σM / σR

each cone, the following procedure was adopted to get the total number of deuterons scattered into each cone. From the above scattering data and from calculated values of Rutherford scattering, the ratio of actual measured scattering to Rutherford scattering at the angles and energies required were plotted as shown in Fig. 13. It should be noted that the measured scattering is higher than the value obtained from Rutherford scattering alone, the ratio depending on energy and angle. Assuming Rutherford scattering and using the analytical expression for the energy and angular dependence of this scattering cross-section the number of deuterons scattered into each cone was obtained by analytical integration between the angular limits of the cone. Then this number was multiplied by the ratio of measured to Rutherford cross-sections for the angle and energy involved in the cone to obtain an approximate value for the actual number scattered into each cone. Now although the cone is symmetrical about the proton beam direction through the target, the cone is not symmetrical with respect to the target to counter direction except when the counter is at 0°. Since an angular distribution was required from the calculations each cone was divided into 12 "tubes" as shown in Fig. 12b, so that each tube contains $\frac{1}{12}$ of the deuterons in the particular cone. All the deuterons in each tube were assumed to travel down the center of the tube, and for each tube the angle between this direction and the line joining the target to the detector was obtained using the methods of solid geometry. These angles were computed for the counter at four different angles, namely at 0°, 45°, 90° and 135° with respect to the incident beam direction. Finally each tube was divided into sections along its length such that the energy loss of the deuteron in traversing each section was approximately equal to the difference between the deuteron energies at the outside and the inside of the particular cone. Assuming the stopping power of heavy ice for deuterons was the same as that for protons of the same velocity the data of Wenzel and Whaling (1952) was used to compute the stopping power of heavy ice for deuterons as a function of deuteron energy. From this data the thickness, and hence the number of stationary deuterons in each tube-section of the target, was obtained. From various measurements of the angular distribution of d on d neutrons at different bombarding energies Hunter and Richards (1949) have plotted the coefficients as a function of energy for expressing the angular distribution in terms of Legendre polynomials. From this data curves were plotted of the d on d neutron yield as a function of angle for the various energies required for this calculation. Thus knowing the angle between the direction of motion of the scattered deuterons in any tube section and the line joining the target to the counter, the number of neutrons produced by the scattered deuterons passing through the particular tube-section and emitted in the direction of the counter could be evaluated. This number was evaluated for each of the tube-sections for the counter in the four different positions specified above. Finally for each of these counter positions the total number of neutrons emitted in the direction of the counter was obtained by adding the contributions from all 672 tube-sections. The results are plotted in Fig. 10.

In order to obtain the calculated 0° excitation function given in Fig. 7, the neutron yield at 0° for each of the six layers was extracted from the thick target calculation given above. These values are given in the table below along with the energies of the protons in each layer.

<u>0° neutron yield</u> - <u>neutrons per steradian per millicoulomb</u>

Layer	proton energy Kev	0° neutron yield
A	1500 to 1322	3.25×10^6
B	1322 to 900	7.02×10^6
C	900 to 563	1.55×10^6
D	563 to 338	1.08×10^5
E	338 to 113	1.08×10^4
F	113	neglected

From this table the thick target yield of neutrons as a function of energy can be easily obtained by adding the 0° contributions from the bottom of the table to the layer which has an incident proton energy equal to the particular energy at which the total yield is required. Thus the 0° thick target yield for 900 Kev incident proton energy is equal to the sum of the contribution from layers F, E, D and C. In this manner the calculated yield points of Fig. 7 were obtained.

The calculation for the thin target yield and angular distribution consisted of essentially a repetition of the thick target calculation but for one layer only with the added complication that it was necessary to take into account the escape of some of the scattered deuterons from the back of the thin ice layer. Since many of the higher energy scattered deuterons escaped from the thin target it was necessary in this case to consider the contributions from low energy scattered deuterons more thoroughly than was necessary for the thick target case. The contribution to the neutron yield from the scattered deuterons in energy range from 100 Kev to 15 Kev was obtained by folding the curve representing the number of scattered deuterons as a function of energy, obtained from the Rutherford formula, with the curve representing the $D(d,n)He^3$ neutron yield (Bretscher, et al 1948), as a function of energy. In this energy range the Rutherford formula is sufficiently close to the measured scattering cross-section that its use should involve only a small error. The contribution from the scattered deuterons of energy less than 15 Kev was neglected.

Chapter V

DISCUSSION

In the calculations described above a number of approximations have been made concerning the proton energy in each layer, the deuteron energy in each section, and the angular distribution of the scattered deuterons. Also it has been assumed that the scattered deuterons travel in straight lines without further scattering. The latter assumption is reasonably good since for the energy concerned the deuterons lose most of their energy by ionization. In the thin target yield measurement the greatest uncertainty arises from the possible error in the target thickness measurements. Further an error which is difficult to estimate may have been introduced by the method used to find the total number of deuterons in each cone. However, the method was used in order to make an analytical integration possible. In spite of the approximation involved it is felt that the calculated results should be correct to considerably better than one order of magnitude and should therefore provide, by comparison with the experimental results, a useful test of the hypothesis on which the calculations were made.

The fact that the neutron yield is proportional to the square of the D_2O concentration as shown in Fig. 11 provides a strong confirmation of the double process nature of the neutron yield. However, it does not provide any information concerning the nature of the double process. The agreement between the calculated and the experimental yield and angular distribution for both thin and thick targets as shown in Fig. 9 and 10, is sufficiently good to confirm the postulated nature of the double process. The hypothesis is further confirmed by the good agreement between the calculated and the experimental excitation functions shown in Fig. 7.

It may at first sight seem strange that the anisotropy in neutron yield appears to be greater for the thick target than for the thin one. However, this can be explained by the fact that the major contribution both to the yield and to the anisotropy is produced by the highest energy scattered deuterons. In the case of the thin target with 1.5 Mev incident protons most of the high energy scattered deuterons escape from the ice layer so that a greater percentage of the neutron yield comes from low energy scattered deuterons for which the neutron yield is nearly isotropic.

BIBLIOGRAPHY

References given in the text by author's name and year of publication are listed alphabetically below:

Arnold, W.R., Phillips, J.A., Sawyer, G.A., Stovell, E.J. and Tuck, J.L. (1952). Phys. Rev. 88, 159.

Bailey, C., Blair, J.M., Kratz, H.R., Sherr, R. and Taschek, R.F. (1947). Phys. Rev. 72, 670.

Beiduk, F.M., Pruett, J.R. and Konopinski, E.J. (1950). Phys. Rev. 77, 622.

Bell, P.R. (1948). Phys. Rev. 73, 1405.

Bennett, W.E., Mandeville, C.E. and Richards, H.T. (1946). Phys. Rev. 69, 418.

Bretscher, E., French, A.P. and Seidl, F.G. (1948). Phys. Rev. 73, 815.

Chadwick, J. (1932). Proc. Roy. Soc. A136, 692.

Coon, J.H. and Nobles, R.A. (1947). Rev. Sci. Instr. 18, 44.

Edwards, M.H. (1951). M.A. Thesis, University of British Columbia.

Emmerich, W.S. (1954). Rev. Sci. Instr. 25, 69.

Graves, J.D. and Dyson, J.P. (1949). Rev. Sci. Instr. 20, 560.

Griffiths, G.M. (1953). Ph.D. Thesis, University of British Columbia.

Hanson, A.O. and McKibben, J.L. (1947). Phys. Rev. 72, 673.

Heiberg, S.A. (1954). Ph.D. Thesis, University of British Columbia.

Hirschfelder, J.O. and Magee, J.L. (1948). Phys. Rev. 73, 207.

Hornyak, W.F. (1952). Rev. Sci. Instr. 23, 264.

Hunter, G.T. and Richards, H.T. (1949). Phys. Rev. 76, 1445.

Jennings, B., Sun, K.H. and Leiter, H.A. (1950). Phys. Rev. 80, 109.

Livingston, M.S. and Bethe, H.A. (1937). Rev. Mod. Phys. 9, 268.

Manning, H.P., Huntoon, R.D., Myers, F.E. and Young, V.J. (1942). Phys. Rev. 61, 371.

Neilson, C. (1955). Ph.D. Thesis, University of British Columbia.

Richards, B.R. (1937). Phys. Rev. 51, 810.

Seagondollar, L.W., Esch, K.A. and Cartwright, L.M. (1954). Rev. Sci. Instr. 25, 689.

Segel, R.E., Swartz, C.D. and Owen, G.E. (1954). Rev. Sci. Instr. 25, 140.

Schiff, L.I. (1949). "Quantum Mechanics", McGraw-Hill Book Co.

Taschek, R.F. (1942). Phys. Rev. 61, 13.

Wenzel, W. and Whaling, W. (1952). Phys. Rev. 87, 499.